A. 1-68-89-I
July 20, 1968

TM-151
2610.1
2630.1

FAKE STUDIES OF SOME STRONG AND WEAK INTERACTIONS IN THE 12-FT AND 25-FT BUBBLE CHAMBERS

PART I. NEUTRINO INTERACTIONS

M. Derrick
Argonne National Laboratory

T. O'Halloran
University of Illinois

and

R. Kraemer
Carnegie-Mellon University

Introduction

To help clarify the problem of the parameters of the proposed 25-ft chamber and to provide a basis of comparison between the ANL 12-ft chamber and the proposed 25 ft, we have generated a number of reactions using the program FAKE. Studies of this kind have previously been made by Chinowsky[1] for ν-induced reactions and by Plano[2] for pion interactions. The present work differs from that previously carried out in that more realistic parameters are used for the chambers and a greater range of event types and energies have been generated.

Error Formulae and Chamber Parameters

We do not discuss the derivation of the error formulae used, since the form of the equations is relatively well known, but merely write down the expressions and constants.[3]

Coulomb term

$$\frac{\Delta p}{p} = \frac{1.5}{\cos\lambda\, \ell^{1/2} H\beta}$$

$$\Delta\phi = \frac{0.23\, \ell^{1/2}}{p\beta \cos\lambda}$$

$$\Delta\lambda = \frac{0.23\, \ell^{1/2}}{p\beta}$$

Measuring term

$$\frac{\Delta p}{p} = \frac{1.9\times10^{-3}\, p\epsilon}{\ell^2 H \cos\lambda}$$

$$\Delta\phi = \frac{3.8 \times 10^{-4}\, \epsilon}{\cos\lambda}$$

$$\Delta\lambda = \frac{3.0 \times 10^{-4}\, \epsilon \cos\lambda}{\ell} \sqrt{1 + \frac{\tan^2\lambda}{9}}$$

Floors were put on λ and ϕ of values:

12-ft chamber		25-ft chamber	
$\Delta\phi$	$\Delta\lambda$	$\Delta\phi$	$\Delta\lambda$
0.9×10^{-4} rads	1.5×10^{-4} rads	0.7×10^{-4} rads	1.1×10^{-4} rads

where:

ℓ = track length in cms

H = magnetic field in kG

p = momentum in MeV/c

ϵ = setting error in space in microns

ϕ = azimuthal angle

λ = dip angle

β = v/c.

Chamber Parameters

The 12-ft chamber was taken to be a cylinder of radius 2 m and depth 2 m, which is approximately the dimensions of the real ANL chamber. For the 25-ft we scaled things to a radius of 4 m and depth of 3 m. This was done for convenience and not because we felt that a pillbox-shaped

chamber is best. The difference between this and the football shape proposed by BNL should not be of any consequence.

The setting error in space (ϵ) for the 12-ft chamber is taken as 250μ. The appendix[4] to the report written by M. Derrick and R. Kraemer lists the different contributions to the point-reconstruction accuracy for the 12-ft chamber. The error is dominated by thermal turbulence of the liquid hydrogen which multiple scatters the rays of light travelling from the bubble to the camera lens. This effect varies as the distance to the 3/2 power as is characteristic of a multiple scattering. It also varies almost linearly with the heat flux through the visible volume of the chamber.[4] Assuming the same heat flux, then the setting accuracy in the 25 ft will be two to three times worse than in the 12 ft since the 25-ft chamber as presently proposed[5] is about twice as deep as the 12 ft. It is also an empirical fact that with chambers presently in use the setting error scales with the chamber size although there are significant variations between chambers of roughly the same size but of different designs. We, therefore, use 250μ for the 12-ft chamber and 500μ for the 25 ft as best guess setting errors. The other two cases we consider are a magnetic field of 40 kG on the 12-ft chamber and an optimistic setting error of 250μ for the 25-ft chamber, giving a total of four different parameter sets listed later.

Neutrino Interactions Generated

We consider the problem of separating the elastic neutrino events:

$$\nu + n \rightarrow \mu^- + p, \qquad (1)$$

from the same reaction with an additional π^o. Since the inelastic channel is dominated by $N^*(1238)$ production, we generated the reaction

$$\nu + n \rightarrow \mu^- + N^{*+} \hookrightarrow p + \pi^o. \qquad (2)$$

The resulting final state $\mu^- p \pi^o$ is not over-constrained since the ν momentum is not known for any individual event, so one can only obtain a 0c solution. The events were generated with a peripheral angular distribution similar to that expected from the known form factors. The distribution actually used was $d\sigma/dt \propto e^{4t}$, with t in $(GeV/c)^2$. The beam was spread out over the whole width of the 12-ft chamber but restricted in depth to the center of the chamber. Some events should perhaps be generated at other depths. For the 25-ft chamber the beam width was not changed, so only the central 4 m were illuminated by the ν beam.

ν Spectrum

Two ν spectra were used. First, a white spectrum typical of a wide-band beam was generated. Figure 1 shows the ν spectrum represented by the 500 events used in this part of the study. It peaks at about 4 GeV and goes up to 20 GeV. Second, a typical narrow-band spectrum peaking at 10 GeV was used, as shown in Fig. 3.

A total of 16 different sets of data, each consisting of 500 events, were generated with the following chamber parameters:

	Chamber	Field	Setting Error
1	12 ft	20 kG	250μ
2	12 ft	40 kG	250μ
3	25 ft	40 kG	250μ
4	25 ft	40 kG	500μ

and the two spectra:

1) white and 2) monochromatic,

and the two event types:

1) elastic reaction (1) and 2) inelastic reaction (2).

Results of FAKE

Figures 2 and 3 show the muon spectra resulting from the two ν spectra for the elastic events. It is clear that the muon spectrum follows the ν spectrum quite closely, which comes from the fact that the reactions are peripheral. Figure 4 shows the proton momentum spectrum from the elastic events. The proton spectra do not depend strongly on the ν spectrum but only on the reaction type and momentum transfer dependence. For the elastic events most protons are below 1 GeV/c and, so, will come to rest in the bubble chamber. With deuterium in the chamber a large fraction of the protons will interact before stopping or leaving the chamber, but this is not of major importance since the momentum is low and well measured with only a small length of proton track.

The angular distribution of the protons is quite different for the N^* and elastic events as seen in Fig. 5. The elastic protons tend to come

out near 90° to the beam direction, although the $\mu^- \nu$ mass difference restricts the maximum proton angle slightly, whereas the protons from the N^* decay have a quite different angular distribution.

These factors all enter into the transverse momentum unbalance shown in Figs. 6 and 7. The measurement accuracy is such that even for the 12-ft chamber with 20 kG and a 10-GeV ν beam the transverse momentum balance is good to approximately 15 MeV/c for the elastic events, whereas for the N^* production a more typical value is 200 MeV/c which represents mainly the transverse momentum of the π^o.

Two important effects are not included in the P_T unbalances shown in Fig. 6. The first is the Fermi motion in the deuteron. In small chambers one can measure a spectator proton if its momentum is less than 80-100 MeV/c. The new chambers will probably be worse than this because of the relatively poor space resolution. Since the spectators are isotropic, the invisible spectator events will give an average P_T uncertainty of approximately 40 MeV/c. The uncertainty in the direction of the ν which is typically a few mrads will add a comparable uncertainty; i.e., $P_\nu \cdot \theta_\nu \sim 10 \text{ GeV} \cdot 3 \cdot 10^{-3}$ or 30 MeV/c for the monochromatic beam. The conclusion is that measuring error in the bubble chamber is not very important for this class of event, so one can use the full length of both the 12-ft and 25-ft chambers for the interaction volume.

Results of Kinematic Fitting

About 100 events in each of the 16 cases have been fit using GRIND.

In generating the events the ν-beam direction was fixed and only the momentum was varied for each event according to the spectra shown in Figs. 1 and 3. Both the momentum and angles of the secondary tracks were smeared within the errors. In fitting the events for the white spectrum the momentum was considered unmeasured, whereas the azimuth and dip-angle errors were fixed at 5 mrad.

The elastic events always gave a satisfactory 3c fit for all chamber and beam combinations. The probability distribution was not uniform, but biassed towards higher probabilities because of the beam angle errors. The fitted values did not vary significantly between the worst (12 ft, 20 kG, 250μ) and the best (25 ft, 40 kG, 250μ) conditions. Table I gives the parameters for a typical event.

For the white spectrum no event generated as $\mu^- N^{*+} \rightarrow \mu^- p \pi^o$ gave a fit to the elastic hypothesis $\mu^- p$ even in the 12-ft chamber with 20 kG. With the monochromatic spectrum, which is essentially a 10-GeV ν beam, two N^* events with very short muon tracks 0.9 cm and 15.1 cms respectively gave fits to the elastic hypothesis but neither would fit the remaining three chamber parameter sets since for those cases the muon momentum was better determined.

An important conclusion from these studies is that the tighter ν momentum provided by the narrow-band beam is not needed for the kinematics. The narrow-band beam then only reduces the overall ν flux and with it the background in the chamber.

Many of the elastic events also gave a 0c solution with an additional

π^o. For both ν spectra and for all chamber parameters almost exactly one-half of the elastic events gave such a 0c solution. The events are easy to separate from the events with a real π^o production, since the pseudo π^o's all go in the direction of the ν beam, as is intuitively obvious, whereas the π^o distribution from the N^* events is approximately isotropic. It is clear that for the events considered here the 0c solution for the elastic events is no problem.

In general this ambiguity will always exist, and, so if there is a class of events which give a π^o in the forward direction, downstream γ-conversion plates would be needed to sign the real events. The design of the 25-ft chamber should take that into account.

Figure 8 shows the end points of the tracks (including the ν interaction point) for the white spectrum in the 25-ft chamber. Most of the muons are swept out of the side of the chamber. If one plans to use spark chambers to label the tracks as hadron or lepton, then access to the chamber will be needed at the side as well as the end.

Conclusion and Possible Further Studies

This report covers the most copious kind of event which bears on the form factor question and concludes that both the 12-ft and 25-ft chambers have plenty of precision. One could extend the immediate study to higher energies, but things will probably vary rather slowly, since the momentum transfer distribution is expected to depend only weakly on the ν energy and in this work is considered to be independent of energy.

When real data of the interactions of ν and $\bar{\nu}$ on free nucleons are available from ANL and BNL, one can use this data to extrapolate to NAL and the 25-ft chamber to make a more realistic simulation.

The problems seem to be more in the beam and backgrounds in the chamber rather than in the basic precision of the device, which is clearly more than adequate.

REFERENCES

[1] W. Chinowsky, 200-BeV Accelerator: Studies in Experimental Use, Lawrence Radiation Laboratory UCRL-16830, Vol. II, 1965, p. 53.

[2] R. J. Plano, op. cit., Vol. III, 1966, p. 256.

[3] R. L. Gluckstern, Nucl. Instr. and Methods, 24, 321 (1963).

[4] L. R. Turner, Limits of Track Location Determination in the 12-ft HBC, ANL-BBC-110 (unpublished).

[5] 25-Ft Cryogenic Bubble-Chamber Proposal, Brookhaven National Laboratory BNL-12400, 1968.

Table I. Elastic Neutrino Event in 12-Ft and 25-Ft Chambers.

Masses in GeV, Momenta in GeV/c, Angles in radians, Lengths in cms

12-ft Chamber 20 kG 250μ

FITBANKS		TRK	P	DIP	PHI	DP	DDIP	DPHI	L	DL
1	0.1057	1	9.1293	0.0503	0.0133	0.0554	0.0005	0.0008	241.59	0.06
2	0.9383	2	0.4953	-1.2130	5.5620	0.0188	0.0120	0.0478	74.85	0.20

FIT NOPT 1 NOTR 3 TYP 1010 HYP 1 ER14 NONE ER15 NONE CHISQ 1.33 ND 3 PROB 0.7228 STEP 2

						Unfitted Values and Errors						Fitted Values and Errors					
TRACK		MASS	CODE	BUB	ION	P	DIP	PHI	DP	DDIP	DPHI	P	DIP	PHI	DP	DDIP	DPHI
A0	0	0.0000	UWWF	10	K	9.245	0.000	3.142	0.000	0.005	0.005	9.231	-0.000	3.142	0.052	0.000	0.000
A3	+	0.9383	WWWF	99	K	0.485	-1.213	5.562	0.004	0.012	0.048	0.487	-1.207	5.563	0.004	0.008	0.023
A2	-	0.1057	WWWF	10	K	9.129	0.050	0.013	0.055	0.001	0.001	9.113	0.050	0.013	0.052	0.000	0.001

25-ft Chamber 40 kG 250μ

FITBANKS		TRK	P	DIP	PHI	DP	DDIP	DPHI	L	DL
1	0.1057	1	9.0997	0.0506	0.0125	0.0139	0.0007	0.0009	618.62	0.06
2	0.9383	2	0.4907	-1.2130	5.5620	0.0113	0.0124	0.0493	74.85	0.20

FIT NOPT 1 NOTR 3 TYP 1010 HYP 1 ER14 NONE ER15 NONE CHISQ 0.57 ND 3 PROB 0.9042 STEP 2

						Unfitted Values and Errors						Fitted Values and Errors					
TRACK		MASS	CODE	BUB	ION	P	DIP	PHI	DP	DDIP	DPHI	P	DIP	PHI	DP	DDIP	DPHI
A0	0	0.0000	UWWF	10	K	9.215	0.000	3.142	0.000	0.005	0.005	9.217	-0.000	3.142	0.014	0.000	0.000
A3	+	0.9383	WWWF	99	K	0.485	-1.213	5.562	0.004	0.012	0.049	0.486	-1.211	5.574	0.004	0.008	0.025
A2	-	0.1057	WWWF	10	K	9.100	0.051	0.012	0.014	0.001	0.001	9.099	0.050	0.012	0.014	0.000	0.001

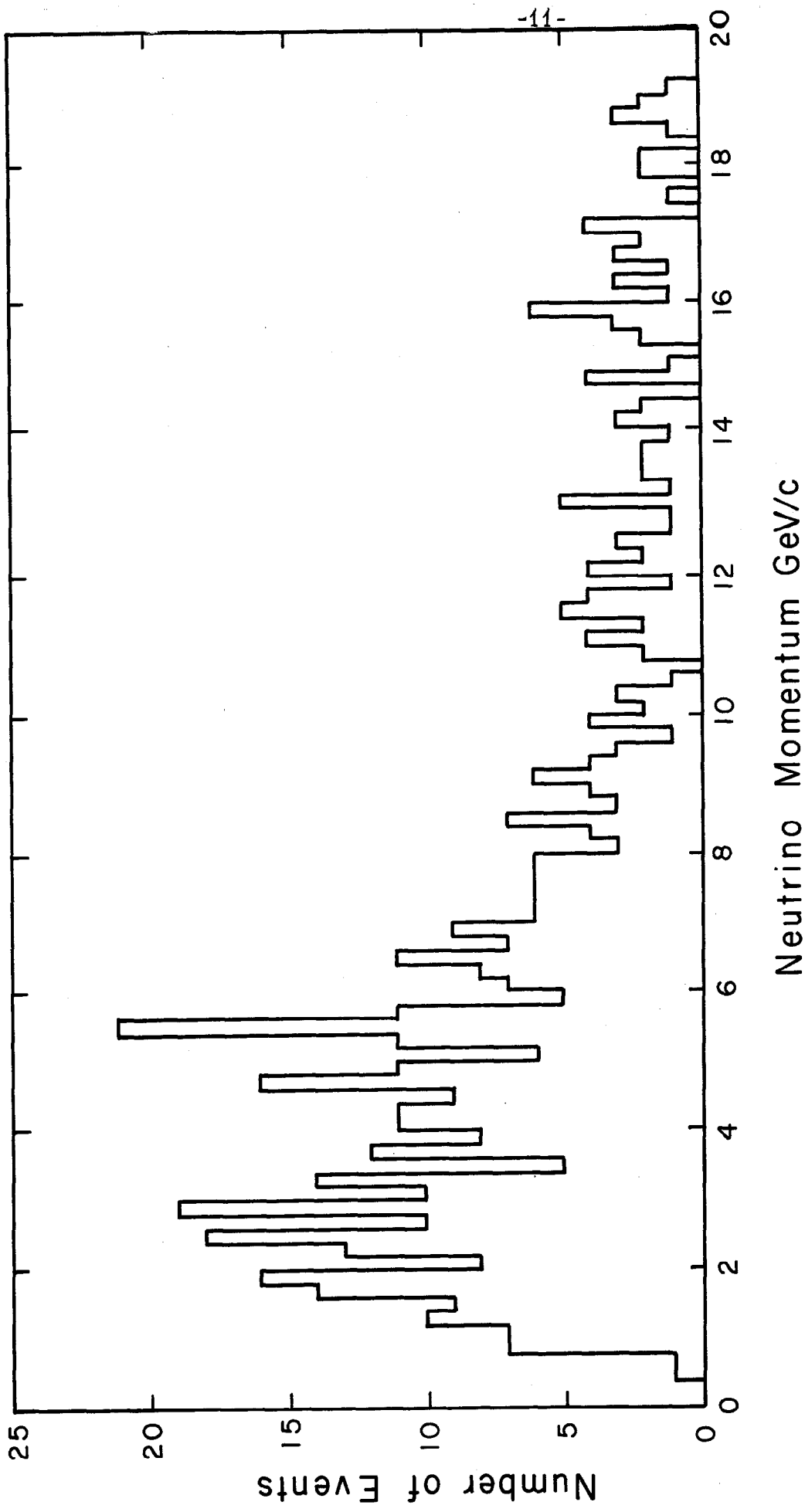

Fig. 1. White neutrino momentum spectrum.

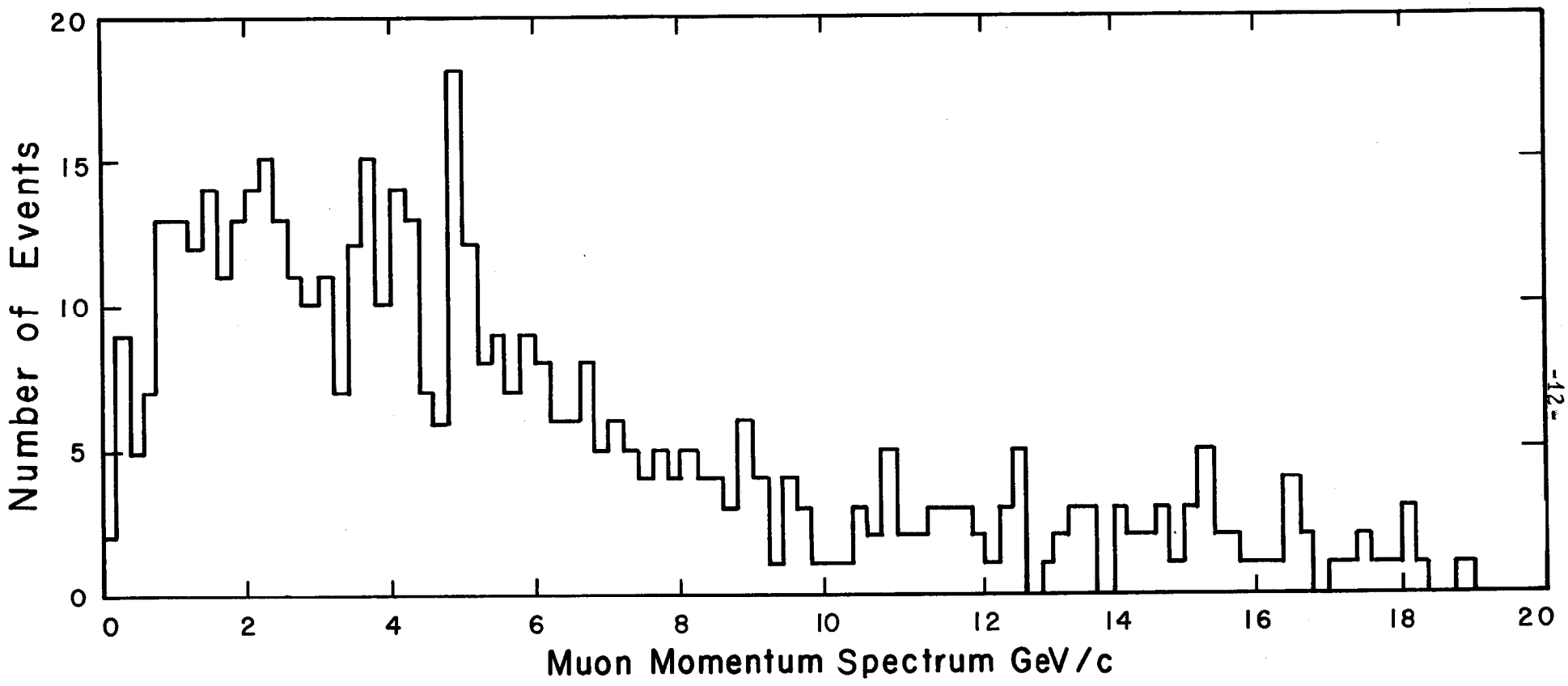

Fig. 2. Muon momentum spectrum from elastic event $\nu + n \rightarrow \mu^- + p$, using white neutrino spectrum.

TM-151
2610.1
2630.1

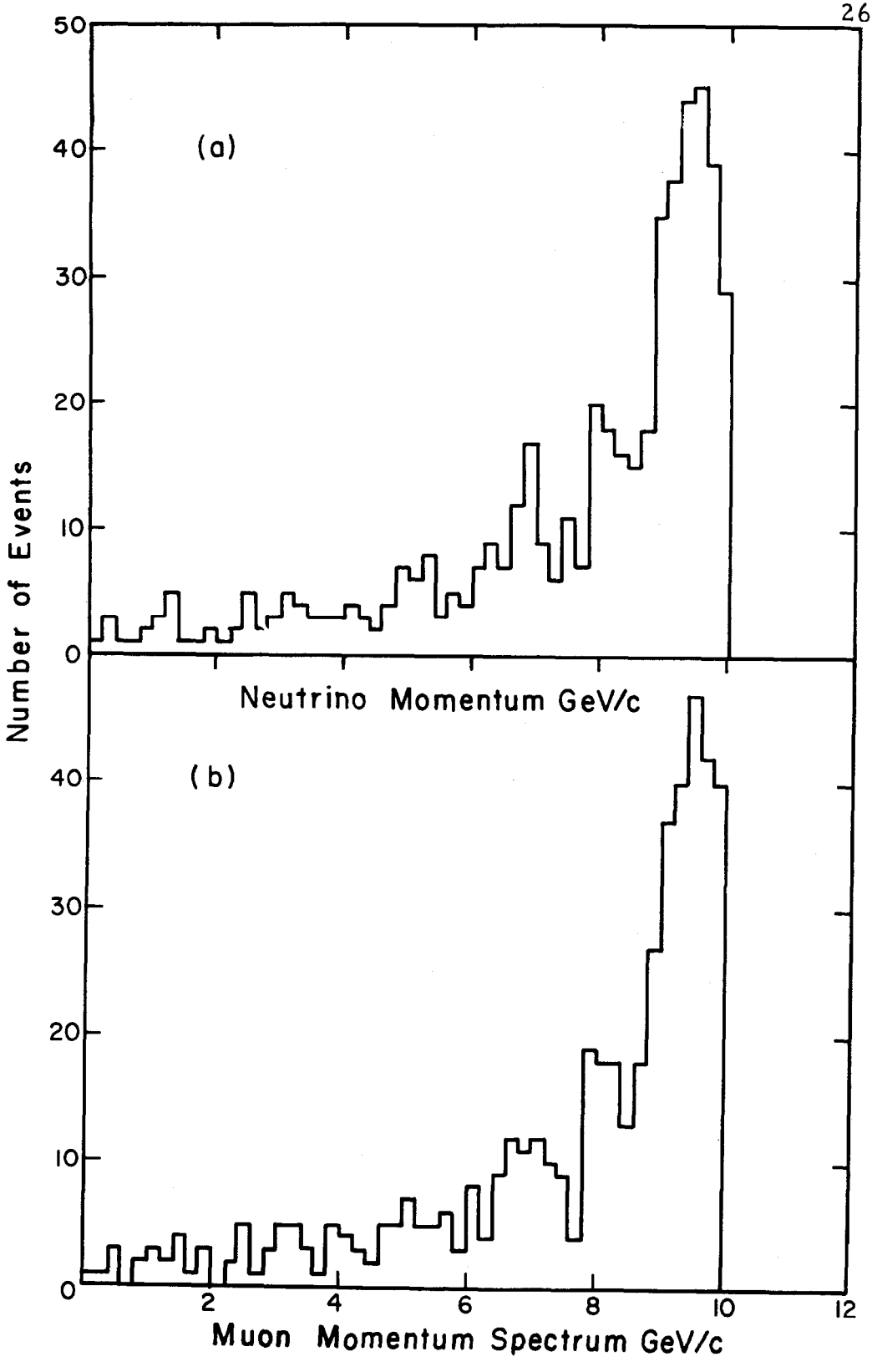

Fig. 3(b). Muon spectrum resulting from elastic scattering of the narrow-band neutrino spectrum of Fig. 3(a).

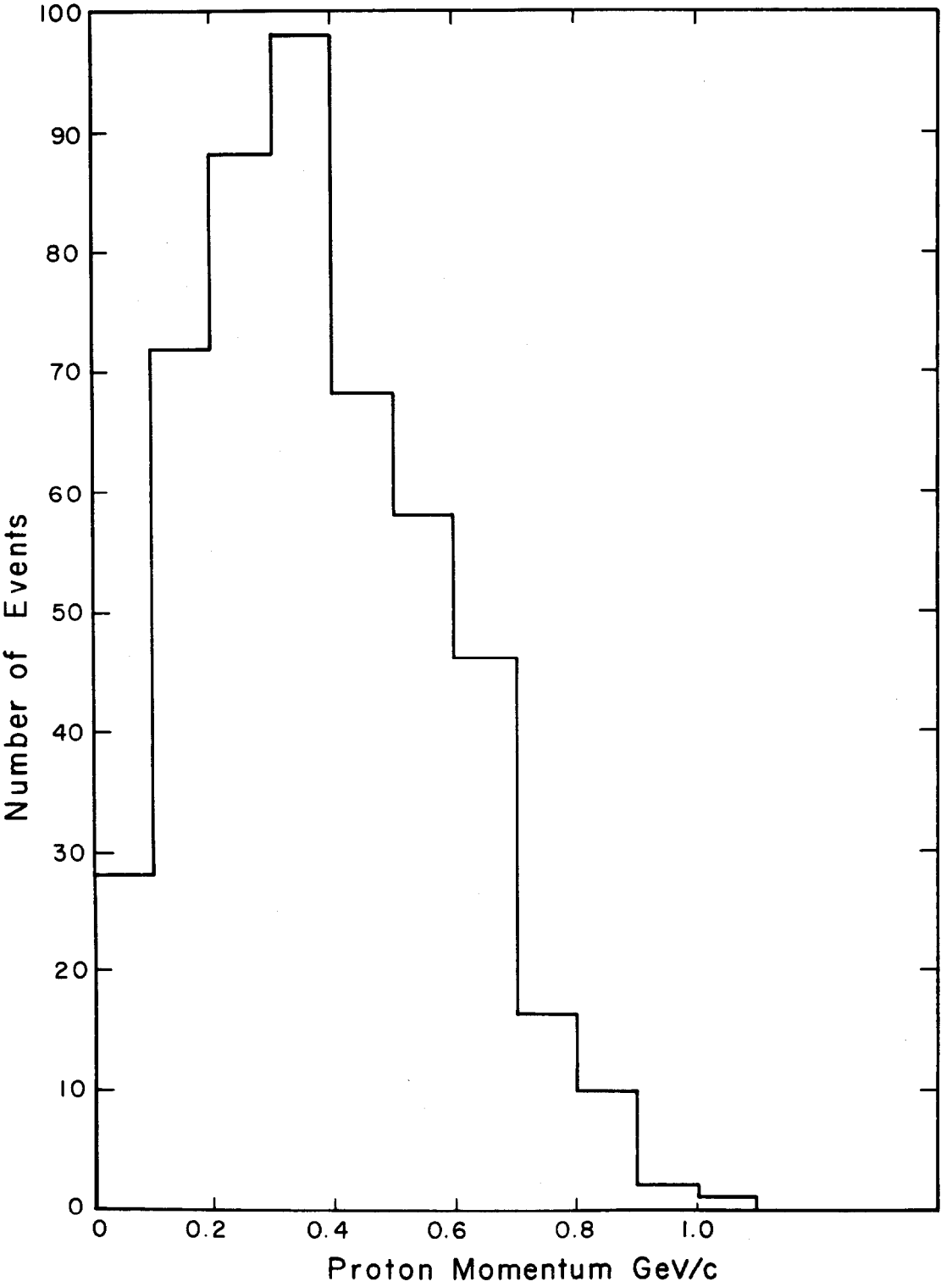

Fig. 4. Elastic proton spectrum from $\nu + n \rightarrow \mu^- + p$ with narrow-band neutrino spectrum of Fig. 3(b).

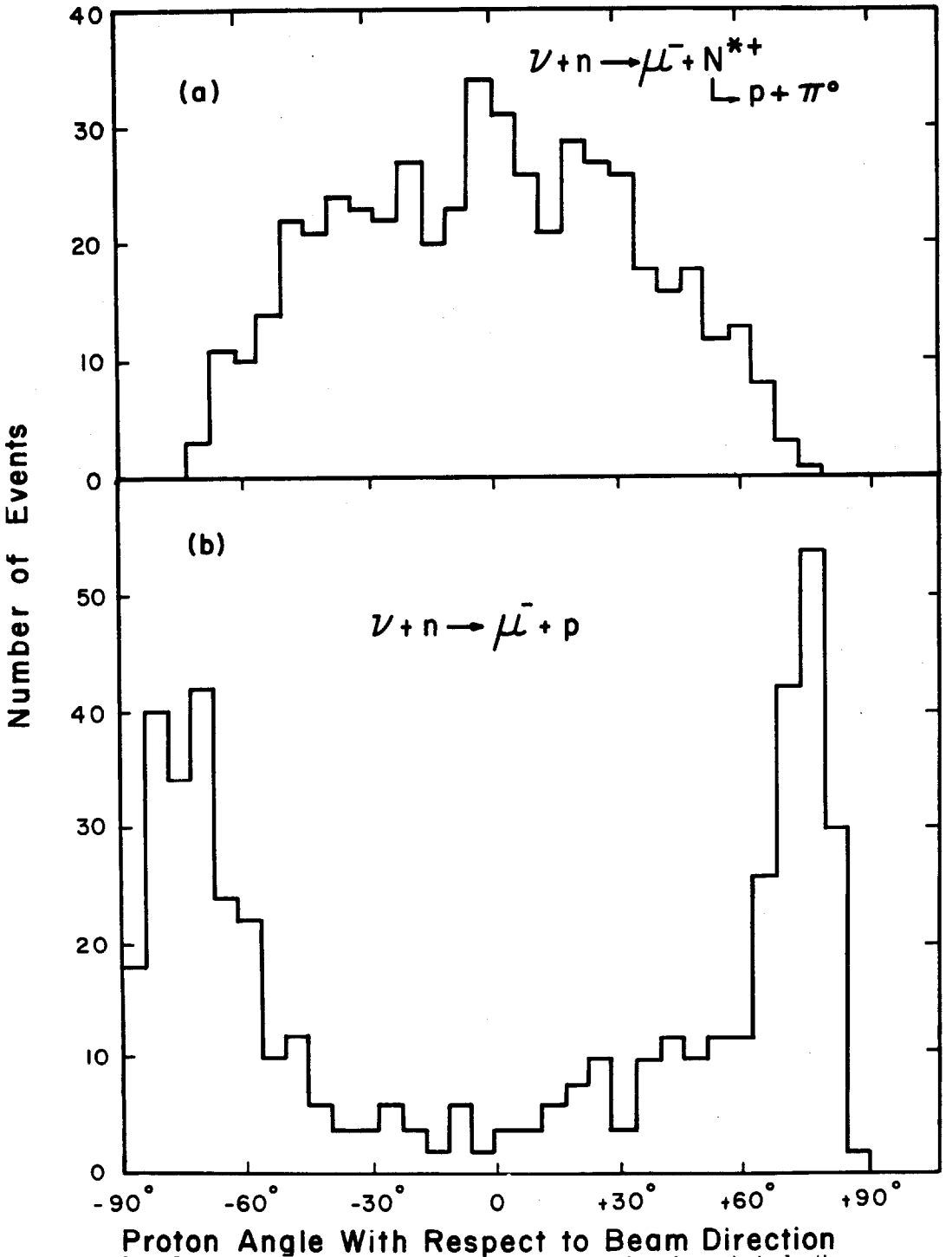

Fig. 5(a). Angular distribution of protons from isobar decay in inelastic reactions; (b) Angular distribution of elastic protons.

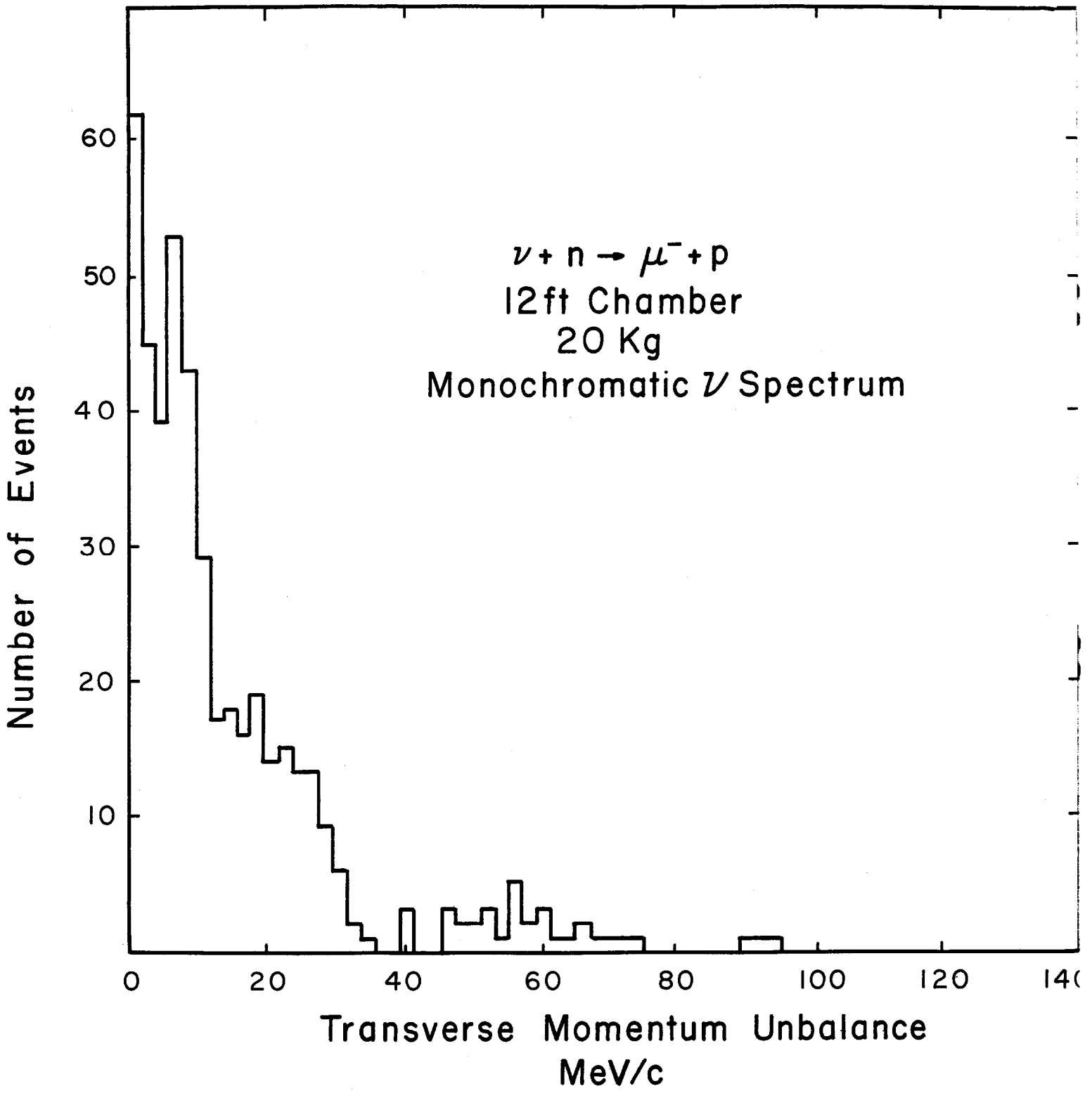

Fig. 6. Missing transverse momentum for elastic events.

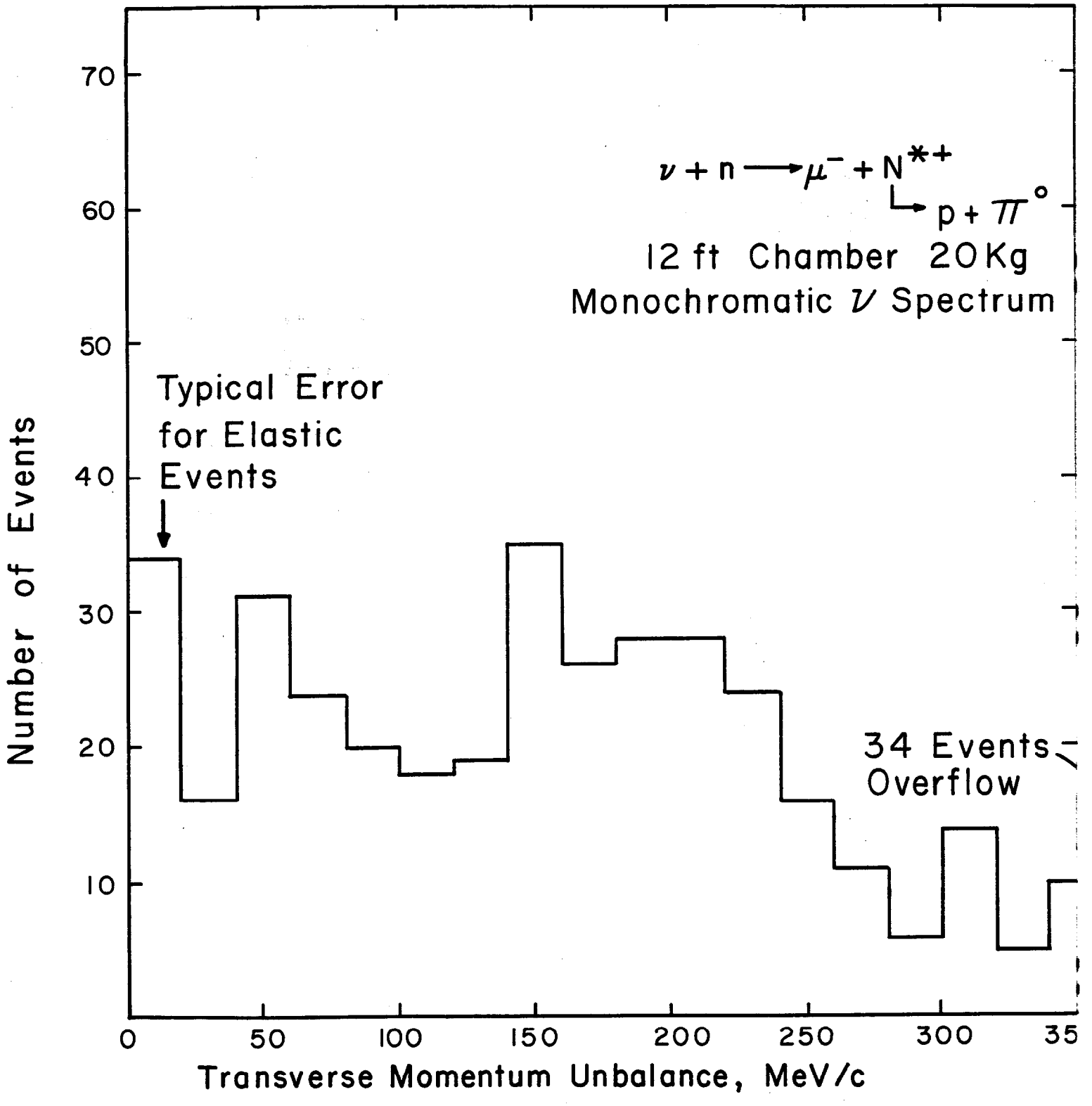

Fig. 7. Missing transverse momentum for inelastic events.